Journal of Catalysis **181,** 113–123 (1999)
Article ID jcat.1998.2283, available online at http://www.idealibrary.com on IDEAL®

Characterisation of Catalysts Used in Wall Reactors for the Catalytic Dehydrogenation of Methylcyclohexane

S. Tschudin,* T. Shido,† R. Prins,† and A. Wokaun*,†

**Paul Scherrer Institut, CH-5232 Villigen, Switzerland; †Department of Industrial and Engineering Chemistry,*
Swiss Federal Institute of Technology, ETH-Zentrum, CH-8092 Zürich, Switzerland

Received June 17, 1998; revised September 10, 1998; accepted September 18, 1998

The catalytically active coatings of tube wall reactors, consisting of an aluminium oxide washcoat and platinum, platinum/tin, or platinum/rhenium deposited by incipient wetness impregnation, are characterized using BET surface area measurements, CO chemisorption, X-ray photoelectron spectroscopy, plasma atomic emission spectroscopy, high resolution transmission electron microscopy (HRTEM), and extended X-ray absorption fine structure analysis (EXAFS). The mesoporous catalysts show a type-IV adsorption isotherm, yielding an average pore diameter of 9 nm, and a BET surface area between 178 and 197 m^2/g. From the bulk and surface analysis results, an enrichment of tin or rhenium, respectively, is found to take place at the surface of the bimetallic catalysts. Very good agreement between the particle sizes estimated from EXAFS, CO-chemisorption, and HRTEM data is found for a low loading (1.5 wt%) platinum catalyst, leading to dispersion values between 75 and 80%, a cluster size of 30 atoms, and a particle diameter around 13 Å. Using the catalytic dehydrogenation of methylcyclohexane as a test reaction, it is demonstrated that a pretreatment at high reduction temperatures leads to a decrease in activity. EXAFS show that this effect is due to a stronger metal–support interaction, as indicated by the appearance of a Pt-O contribution at 2.25 Å in the coordination sphere of the surface platinum atoms.

INTRODUCTION

The catalysts investigated in this study are used in a project aimed at the seasonal storage of electric energy. In view of spatial and temporal mismatch between production and demand of energy, the need for storage, long distance transport, and distribution of energy is a well-recognised problem. Solutions offering the possibility of long-term storage with minimum transport losses are in the centre of interest. Several projects (1–5) deal with the seasonal storage and transport of surplus electricity, produced during summer time out of hydropower. For the optimum use of renewable energy sources, such as solar energy or wind power, efficient storage solutions will again be a prerequisite.

One of these solutions is the so-called MTH cycle (methylcyclohexane, toluene, and hydrogen) first proposed by Taube and Taube (6). In this cycle surplus summer electricity is used to produce hydrogen by electrolysis of water. In a hydrogenation step, hydrogen and toluene are converted into methylcyclohexane. The product methylcyclohexane can be stored at ambient pressure in tanks for a long period. During winter season with a larger demand for electricity, hydrogen can be recovered from methylcyclohexane by dehydrogenation, and transformed into heat, power, or electricity. Toluene is recycled for further use in the next summer cycle.

For the highly endothermic dehydrogenation reaction ($\Delta H_r^{298K} = 205$ kJ/mol) usually packed bed reactors with catalyst pellets are applied. Methylcyclohexane dehydrogenation has been carried out using monometallic and bimetallic catalysts with aluminium oxide as support. Among the monometallic catalysts, platinum treated with sulphur showed the best results (7). For the bimetallic compositions, Pt-Sn (8, 9) and Pt-Re (10) showed high selectivity, as well as good stability for the methylcyclohexane dehydrogenation. Müller (11) used specially prepared organometallic cluster catalysts and reported high selectivity and activity, comparable with commercial catalysts.

Platinum and bimetallic Pt-M catalysts have been used in the closely related catalytic reforming of naphtha in order to improve the octane number. In this process, the fast dehydrogenation of cycloalkanes to aromatics occurs mainly in the first adiabatic reactor (12).

The use of packed-bed reactors for a fast and highly endothermic reaction, such as the dehydrogenation of methylcyclohexane, results in serious heat transfer problems. Large temperature gradients in packed-bed reactors are usually undesirable for several reasons, i.e. an unfavourable influence on the equilibrium conversion, undesirable effects on the activity, selectivity or physical stability of the catalyst, and, due to their adverse impact on reactor operation, safety. These problems could be avoided by enhancing the heat transfer to the catalyst by the application of wall

0021-9517/99 $30.00

reactors, instead of packed-bed reactors. The design of wall reactors, in which a catalytic coating is applied to the tube wall, results in good temperature control and reduces temperature gradients (13).

In view of the mentioned results reported for packed-bed reactors, we decided to study monometallic Pt, as well as bimetallic Pt-Re and Pt-Sn catalysts, on aluminium oxide support in a wall reactor. As the preparation procedure for the catalytic coatings is largely different from the one of catalyst pellets, an in-depth characterisation was required.

EXPERIMENTAL

Catalyst Coating

Four different catalysts were prepared by Doduco GmbH, by wash coating and impregnation by incipient wetness:

(a) platinum A: 3 mg/cm^2 Pt on γ-Al_2O_3, desired metal loading 1.5 wt%.
(b) platinum B: 3 mg/cm^2 Pt on γ-Al_2O_3, desired metal loading 15 wt%.
(c) platinum/rhenium: 3 mg/cm^2 Pt/Re on γ-Al_2O_3, desired metal loading 0.5/0.5 wt%.
(d) platinum/tin: 3 mg/cm^2 Pt/Sn on γ-Al_2O_3, desired metal loading 0.5/0.5 wt%.

A Fecralloy® tube, a steel tube with a high aluminium content, was used as substrate for the wash coat. Prior to the coating the tube was rinsed with acetone and was heated up to 1273 K for 4 h under 200 ml/min air flow. This procedure results in an enrichment of aluminium on the surface, which proved helpful for attaching the wash coat to the steel tube. The desired amount of the wash coat was applied to the reactor tubes in several dipping and drying steps. Finally, the metal salts were deposited by incipient wetness impregnation.

Catalyst Pretreatment

For the pretreatment of the catalyst two different procedures were used. The first, termed “direct reduction,” consisted of a reduction step at 703 K for 2 h in 30 ml/min of pure hydrogen (99.995%, Sauerstoffwerk Lenzburg AG). The second, termed “mild reduction,” started with a drying step in a 100 ml/min flow of pure nitrogen (99.999%, Sauerstoffwerk Lenzburg AG) while the temperature was increased from ambient to 573 K at a rate of 10 K/min. This was followed by a reduction step in 30 ml/min pure hydrogen at 663 K for 2 h.

Catalytic Tests

The catalytic studies were carried out in a micro reactor system. Prior to the catalytic test one of the above pretreatments was applied. The reactant hydrogen flow was controlled by a mass flow controller, and the hydrogen flow in the product stream after the condenser was determined by a mass flow sensor (Bronkhorst High-Tec F-201C-FA). Methylcyclohexane (impurities <0.2%, EMS Chemie) was fed by a step-motor pump (RTC® M16) and evaporated into the preheated feed gas stream. Hydrogen to methylcyclohexane ratios used in the tests were 5 : 1 and 1 : 1. The pressure in the system was regulated between 2 and 7 bar absolute by a pressure controller (Bronkhorst High-Tec P-702C-FA). The weight hourly space velocity (WHSV) was maintained at 10 h^{-1}. For each set of feed and pressure conditions, catalytic conversion was determined for three temperatures levels, i.e. 598 K, 648 K, and 698 K. The gas composition at the reactor outlet was monitored using a gas chromatograph (Hewlett-Packard, type 5890 series II) with a cross-linked methyl-silicone-gum column (HP1). The establishment of steady-state was verified for all results reported below.

BET Surface Area Measurements

For the BET surface area measurements, the catalyst was scraped from the tube substrate and powdered, to avoid any influence from the steel tube. The BET surface areas were measured by nitrogen (99.999%, PanGas) physisorption at 77 K, using a Micromeritics gas adsorption apparatus (ASAP 2000). Prior to the measurement, the samples were degassed overnight in vacuum at 473 K. For the calculation of the BET surface areas, the relative pressure range p/p_0 of 0.05 to 0.2 was used. The pore radius distribution was determined by the method of Barrett, Joyner, and Halenda (BJH method).

CO Chemisorption

Before the measurement, the samples scraped from the tube walls were pretreated at 623 K for 30 min in oxygen (99.995%, PanGas), cooled down to room temperature, and then heated up to 373 K in helium (99.995%, PanGas). The following reduction step at 623 K in hydrogen (99.995%, PanGas) lasted for 2 h. The carbon monoxide (99.995%, PanGas) chemisorption was carried out in a Micromeritics apparatus (ASAP 2010C) at 308 K.

Inductively Coupled Plasma Atomic Emission Spectroscopy (ICP-AES)

The powdered samples were mixed with potassium pyrosulfate. This mixture was heated with a gas burner and the resulting solid residue was dissolved in dilute sulphuric acid. The resulting solution was analysed using an ARL-3410 analyser.

X-Ray Photoelectron Spectroscopy (XPS) Measurements

The XPS measurements were performed in a Leybold LH 11 XPS apparatus, with the powdered catalyst samples supported on appropriate tabs. A Mg K_α radiation source was used with an energy of 240 W. The analyser had a constant pass energy of 150 eV, and the pressure in the sample chamber was at 5×10^{-9} mbar. The surface composition was determined after the subtraction of a Shirley-type background.

High Resolution Transmission Electron Microscopy (HRTEM) Measurements

The catalyst was examined fresh (without any pretreatment) and after a mild pretreatment. A small amount of the scraped and powdered catalyst was mixed with ethanol. This mixture was put into a ultrasonic bath before it was applied to a special carrier matrix. For the examination a Phillips microscope CM 30 ST (300 kV) was used.

Extended X-Ray Absorption Fine Structure (EXAFS) Measurements

The samples were characterized by EXAFS spectroscopy at the Swiss Norwegian Beamline (SNBL) of the European Synchrotron Radiaton Facility (ESRF) in Grenoble. The storage ring was operated at 6 GeV and a current between 120 and 250 mA. Samples were pressed into self-supporting wafers and placed in an *in situ* cell (14). All pretreatments were carried out *in situ*. EXAFS measurements were performed at the Pt L_3-edge at liquid nitrogen temperature. Data were collected in transmission mode using a Si (111) double crystal monochromator.

The EXAFS spectra were analysed by deglitching, pre-edge subtraction, normalisation, and Fourier transformation of the obtained $\chi(k)$ spectra. The FT-spectra were fitted using standard procedures. Data for the phase shifts and back scattering amplitudes were obtained form reference compounds. Pt foil was used as reference for modelling the Pt-Pt contributions, and $Na_2Pt(OH)_6$ for the Pt-O contributions (15).

RESULTS

BET Measurements and CO-Chemisorption

Results from the nitrogen physisorption and carbon monoxide chemisorption measurements are compiled in Table 1. The physisorption isotherms of all samples showed a type-IV shape, according to the IUPAC classification (16).

TABLE 1

Textural Properties of Catalysts from BET and CO Chemisorption Measurements

Catalyst	BET surface area m^2/g	Pore diameter nm	Metal surface area m^2/g	Dispersion %
Pt A	197	8.9	5.2	76
Pt B	188	9.0	7.6	44
Pt/Sn	178	9.0	0.8	31
Pt/Re	190	9.1	0.1	12

TABLE 2

Metal Loadings from ICPAES and XPS Measurements

	ICPAES		XPS		
Catalyst	Metal 1 wt%	Metal 2 wt%		Metal 1 wt%	Metal 2 wt%
Pt A	2.75		Pt 4d	2.85	
Pt B	6.98		Pt 4d	4.86	
Pt/Sn	0.81	1.16	Pt 4d/Sn $3d^{5/2}$	0.98	2.39
Pt/Re	0.47	0.27	Pt 4d/Re 4f	1.01	0.97

This is typical for porous systems with mesopores between 2 and 50 nm and is often observed for industrial catalysts. The mean pore diameter for the four samples is around 9 nm. With BET surface areas between 178 m^2/g and 197 m^2/g the samples are in the range of commercial catalysts with γ-Al_2O_3 as support. The platinum catalyst A with a comparatively low Pt loading (cf. Table 2) and a specific metal surface area of 5.2 m^2/g shows a good dispersion, while the more heavily loaded Pt B catalyst exhibits a significant decrease in dispersion. The very low metal surface areas and dispersion values for the bimetallic catalysts Pt/Sn and Pt/Re could be caused by the low drying and reduction temperatures below 773 K, as pointed out in Ref. (17).

ICP-AES and XPS Measurements

Results from the ICP-AES and XPS measurements are compiled in Table 2. For catalyst Pt A we note a good agreement between the bulk composition (2.75 wt%) as determined by ICP-AES, and the surface composition (2.85 wt%) from XPS. For catalyst Pt B the difference between the ICPAES and the XPS value is larger, as may be expected from the lower dispersion (Table 1). It is interesting to note that XPS shows a higher loading of the second metal, relative to the values measured with ICP-AES, for both the Pt/Sn and the Pt/Re catalyst.

HRTEM Measurements

In the micrograph of the fresh Pt A catalyst after direct reduction (Fig. 1), only very big metal particles with sizes between 15 nm and 85 nm are discerned. These particles show the typical shapes of face-centred cubic (fcc) crystals as presented by Yacaman *et al.* (17). The authors point out (18) that their population is a function of temperature of reduction and preparation conditions. Figure 1 is also representative for the fresh samples of the other investigated catalysts. From inspection of the HRTEM image in Fig. 1 it is clear that none of the dispersion values in Table 1 would be compatible with particles of the size shown.

Therefore, further HRTEM measurements were carried out with samples that underwent a mild pretreatment as described in the experimental section. The resulting micrograph for the Pt A catalyst is shown in Fig. 2. A mean particle

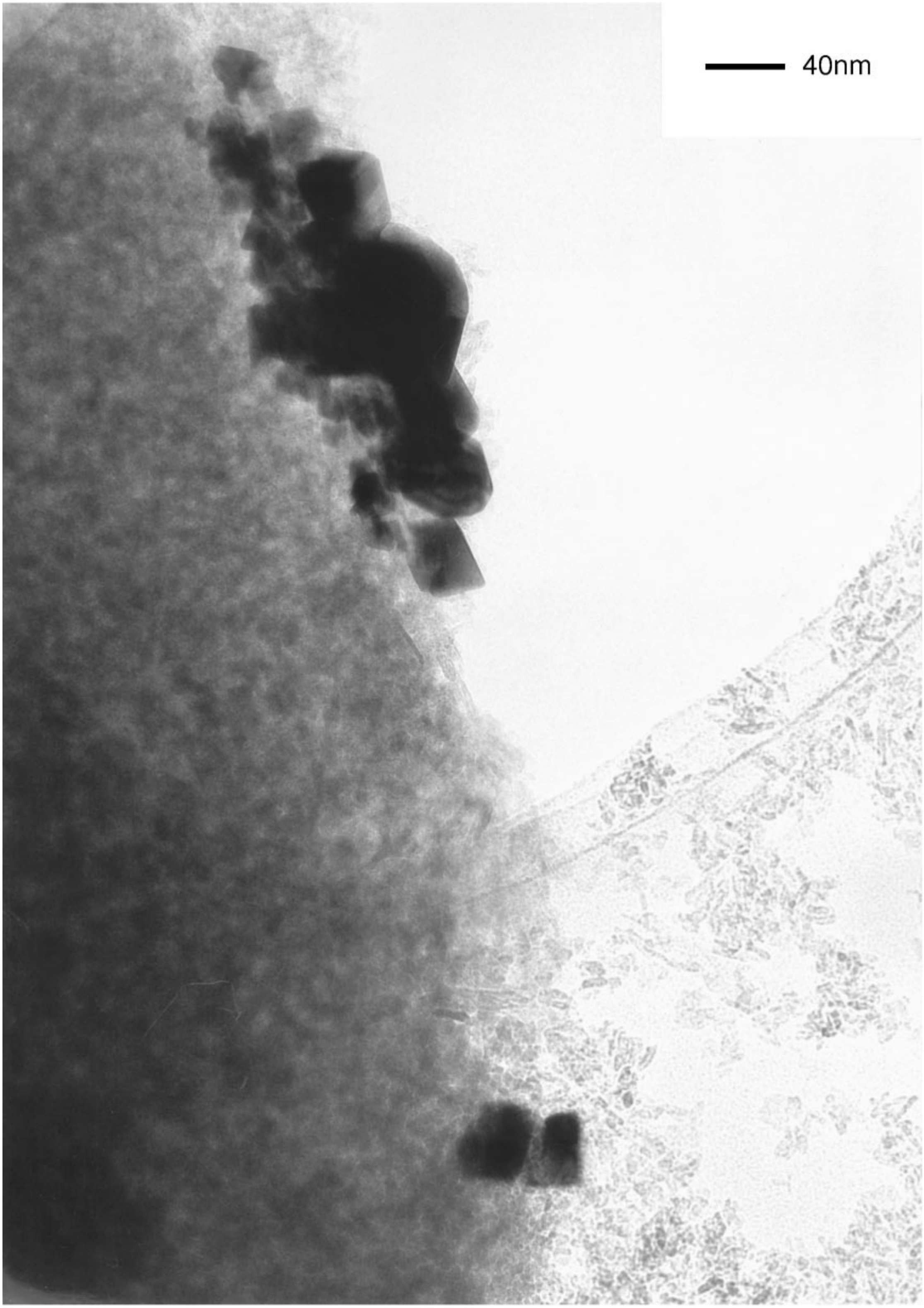

FIG. 1. High resolution transmission electron micrograph of the fresh Pt A catalyst after direct reduction (cf. Experimental part).

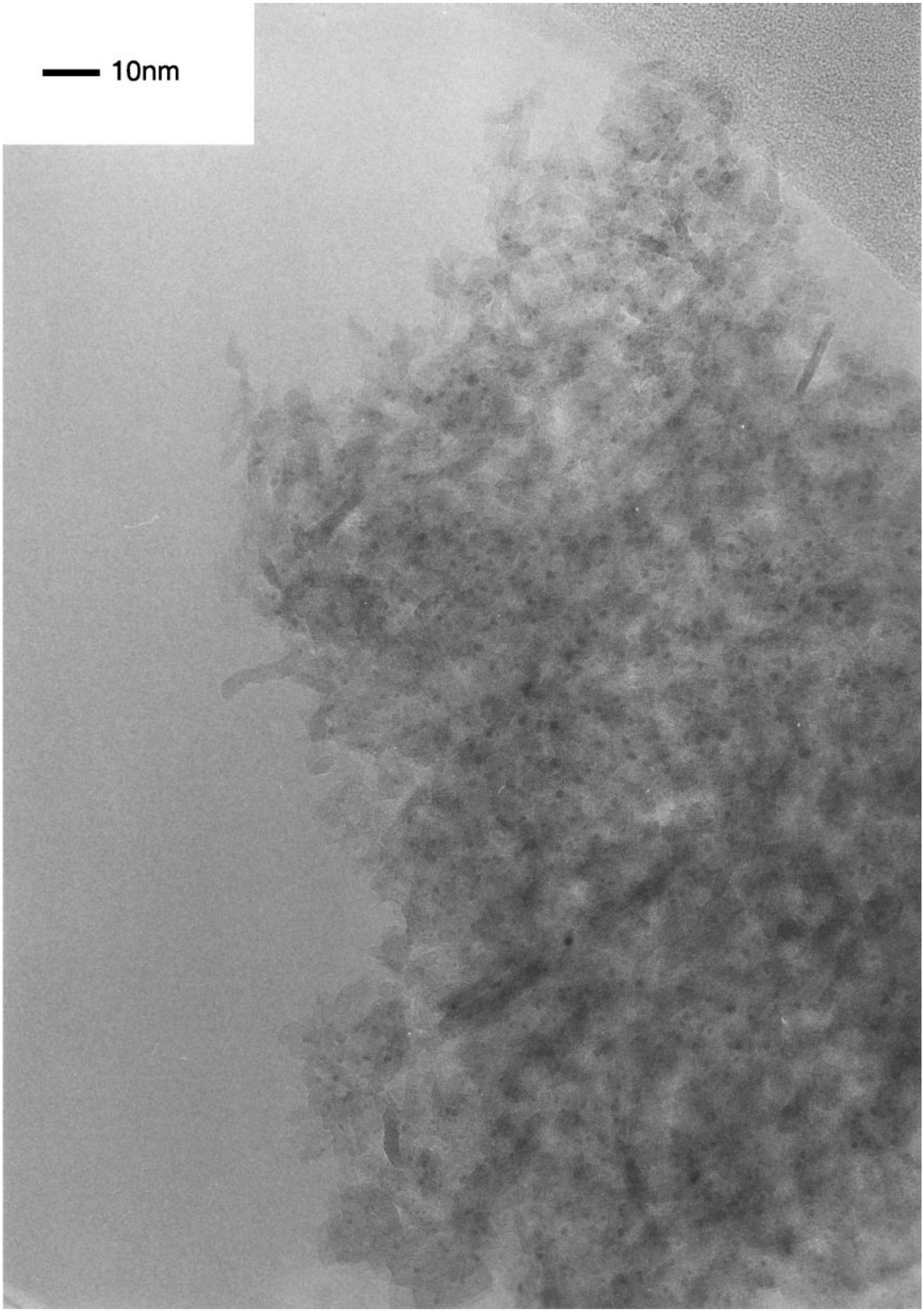

FIG. 2. High resolution transmission electron micrograph of the Pt A catalyst after mild pretreatment (drying at 573 K and reduction at 663 K; cf. Experimental part).

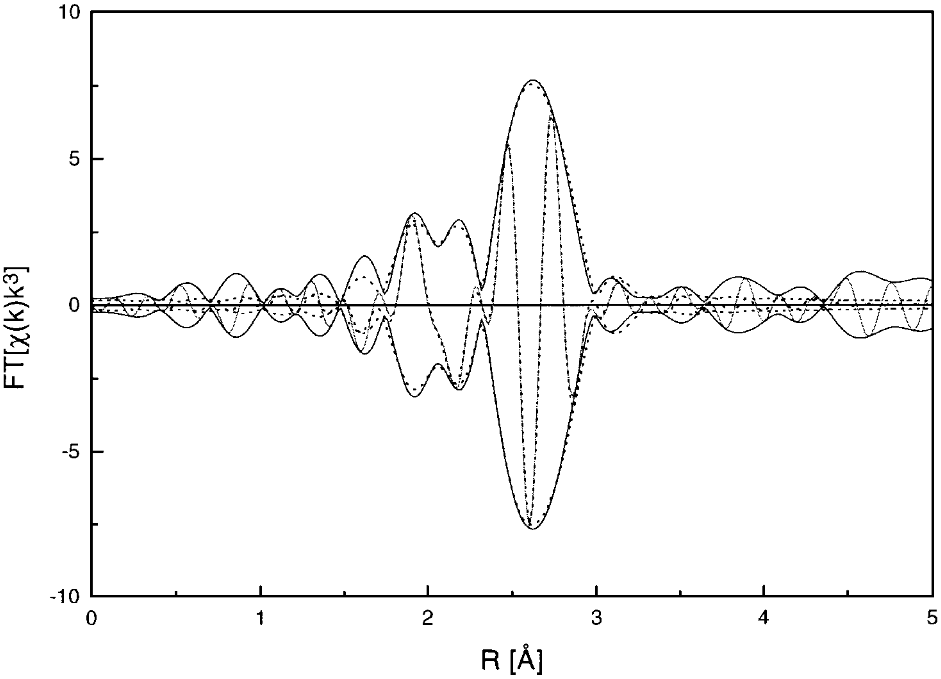

FIG. 3. EXAFS spectra (Fourier transform of $\chi(k)k^3$) of the Pt A catalyst after direct reduction at 703 K (solid line). A fit including both Pt-Pt and Pt-O contributions is shown as a dotted line.

size was determined by measuring 180 particles and by calculating an average diameter. This leads to a mean particle diameter of 13.6 Å. A diameter in the same range (13 Å) was confirmed for Pt catalyst A after 48 h of reaction. Using the mathematical relation between metal loading, particle diameter, and dispersion of supported catalysts derived by Pérez *et al.* (19), a dispersion between 75% and 79% was obtained. This is in good agreement with the chemisorption data.

EXAFS Measurements

Figure 3 shows the Fourier transformed EXAFS spectrum observed with catalyst Pt A after direct reduction at 703 K, as described in the experimental section. The (k^3 weighted) Fourier transform shows a Pt-Pt contribution at 2.6 Å. A second scattering centre besides platinum, which is not present in the spectra of the reference Pt-foil, is observable around 2 Å. The fitting of the Fourier filtered, phase-shift corrected EXAFS spectra resulted in the identification of two significant contributions presented in Table 3. The first is a Pt-Pt contribution at 2.74 Å, with a coordination number of 6.3. The second is a Pt-O contribution at 2.25 Å with a coordination number of 0.7. Similar EXAFS spectra were obtained by Vaarkamp *et al.* (20) after reduction of platinum catalysts at higher temperatures.

The Fourier transformed EXAFS spectrum of the Pt A catalyst after the mild pretreatment at 663 K, as described in the experimental section, is shown in Fig. 4. In the k^3 weighted Fourier transform a Pt-Pt contribution is observable at around 2.6 Å. No other peak deviating form the spectra of the Pt-foil could be detected. This is confirmed by the fitting of the Fourier-filtered EXAFS spectra, with results shown in Table 4. A significant fit of the spectrum was obtained in terms of a Pt-Pt contribution at 2.74 Å and a coordination number of 6.8. The same facts were obtained by Vaarkamp *et al.* (20) for their reduction procedures at temperatures of 573 K.

From the coordination number of this fully reduced state of the Pt A catalyst, the number of atoms per cluster was calculated according to Shido and Prins (21). This calculation is based on the assumption of hemispherical particles. With a coordination number of 6.8 a cluster size of about 30 atoms was derived. This agrees with the findings from

TABLE 3

EXAFS Structural Derived from the Data in Fig. 3

Absorber	Backscatterer	CN[a]	$\Delta\sigma^2$	R/Å
Pt	Pt	6.3	0.0032	2.74
Pt	O	0.7	0.0021	2.25

[a] Coordination number.

TABLE 4

EXAFS Structural Derived from the Data in Fig. 4

Absorber	Backscatterer	CN[a]	$\Delta\sigma^2$	R/Å
Pt	Pt	6.8	0.0032	2.74

[a] Coordination number.

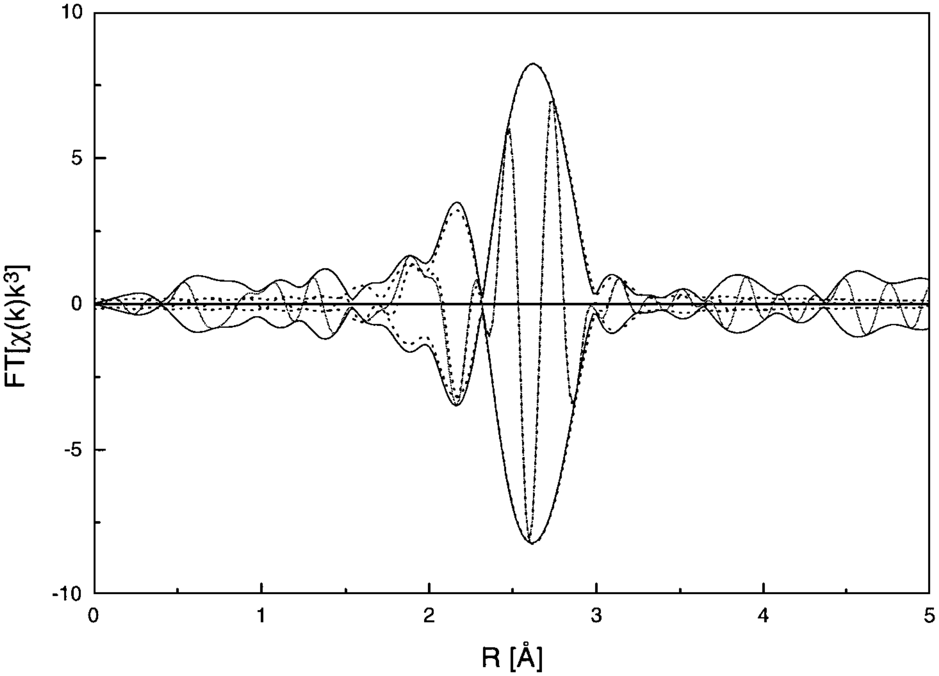

FIG. 4. EXAFS spectra of the Pt A catalyst after a mild pretreatment at 663 K (solid line). A fit including only a Pt-Pt contribution derived from a Pt-foil reference sample is shown as the dotted line.

Kip *et al.* (22) who calculated a diameter of 4.4 times the atomic diameter for a cluster containing 30 atoms. With an atomic radius of 137.3 pm, this leads to a particle diameter of 12.1 Å, in good agreement with the TEM results. If we use the relation between coordination numbers and dispersion derived by Kip *et al.* (22), a dispersion of 80% is determined for a coordination number of 6.8.

An overlay of the Fourier transformed EXAFS spectra recorded after direct reduction and after mild pretreatment is presented in Fig. 5. The small increase in the amplitude

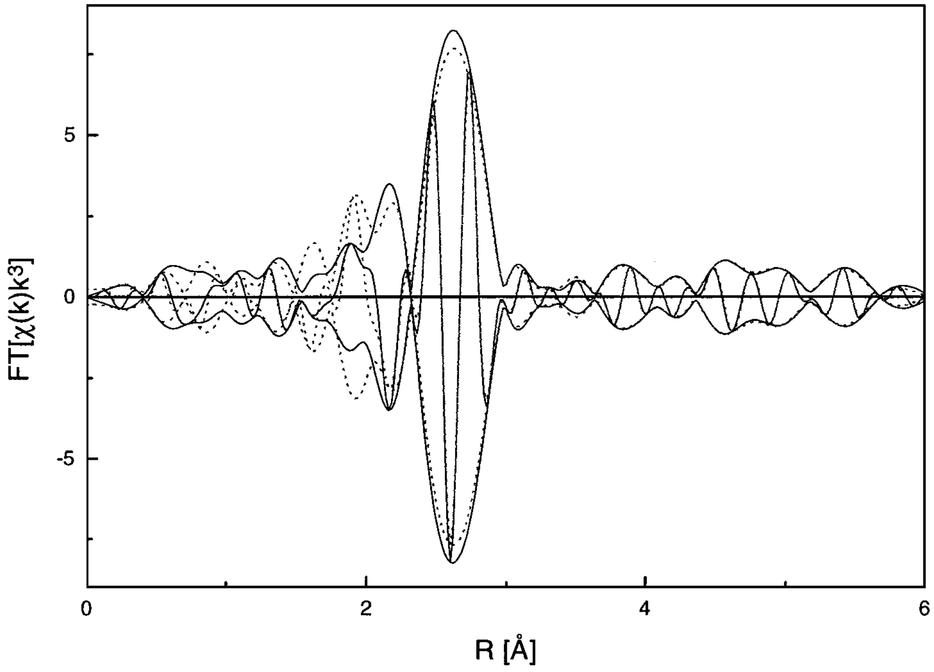

FIG. 5. Overlay of the EXAFS spectra observed after direct reduction at 703 K (data from Fig. 3, dotted line) and after a mild pretreatment at 663 K (data from Fig. 4, solid line).

of the Pt-Pt contribution is also represented in the Pt-Pt coordination numbers in Tables 3 and 4. A coordination peak around 2 Å is observable with the higher reduction temperature (direct reduction). This peak accounts for the Pt-O contribution.

DISCUSSION

Structural Parameters Derived form BET, CO-Chemisorption, ICP-AES, and XPS

The BET measurements show that the textural parameters of the catalysts used in the wall reactors are comparable to those of commercial catalysts used for the dehydrogenation of methylcyclohexane in packed-bed reactors (7, 11). A comparison of the values for the metal loading from ICP-AES and XPS for the platinum catalyst Pt A exhibits a very good agreement between these two methods. Because the former is a bulk and the latter is a surface sensitive method, this indicates that the platinum on this catalyst is well dispersed and present in clusters with a thickness of no more than 10 atom layers. CO-chemisorption measurements confirmed this fact, yielding a dispersion of 80%.

The same comparison, when made for the Pt B catalyst, leads to the conclusion that the metal in this catalyst is not as well dispersed. The loading obtained from the surface method is lower than the one from the bulk method. The corresponding lower dispersion value of 44% resulting from CO-chemisorption is in agreement with this difference.

Of particular interest is the comparison between ICP-AES and XPS for the two bimetallic catalysts. Both show higher metal loading values for the second metal in the XPS measurements. This indicates that tin as well as rhenium are enriched at the catalyst surface, as compared to the platinum. The results from CO-chemisorption show that the low reduction temperatures employed lead to a poor dispersion for the bimetallic catalysts. The low carbon monoxide uptakes may be due to an interaction between the two metal oxide species. Various studies (17, 23, 24) describe such a behaviour for rhenium for low reduction temperatures, as used in the mild pretreatment.

HRTEM Measurements

The high resolution micrographs presented in Figs. 1 and 2 emphasise the importance of the pretreatment. Direct reduction of the unpretreated catalyst (i.e., in the presence of moisture) leads to extensive sintering of the platinum particles, as expected from experience. In contrast, good dispersion is obtained if the reduction step is preceded by drying. The mean particle diameter of 13 Å determined from Fig. 2 is in good agreement with the value of 12.1 Å derived from EXAFS. Similarly, the dispersion for Pt A between 75% and 79% calculated from HRTEM following Pérez *et al.* (19) was confirmed by EXAFS (80%), as well as by CO-chemisorption (76%). The good correspondence between the above three methods does not only provide strong evidence for a true dispersion value around 80%, but also points to a good reproducibility of the catalyst surface with the mild pretreatment, as for each experiment a freshly prepared sample was used.

Dehydrogenation experiments of methylcyclohexane, as mentioned in the experimental section and described in detail elsewhere (25), showed that the well dispersed catalyst Pt A exhibited high catalytic activity, i.e. high toluene yields. These tests also revealed that the degree of dispersion, as established by the pretreatment, does exert a strong influence on the catalytic activity. In the state after direct reduction (Fig. 1) catalyst Pt A is not very active; the same statement holds for the bimetallic catalysts after mild reduction. Significantly higher yields were obtained with the bimetallic catalysts after direct reduction at 703 K, because of an ensuing higher dispersion.

HRTEM pictures of a Pt A sample after 48 h of continuous reaction showed no difference in the particle size. This was also confirmed by EXAFS measurements performed *in situ* under dehydrogenation conditions. Similar experimental results were obtained by Caballero *et al.* (26, 27) with Pt, Pt/Re, and Pt/Sn catalysts.

EXAFS Measurements

Noting that the reduction temperature (703 K) of the sample characterised by the EXAFS spectrum in Fig. 3 was higher than the one (663 K) used for the sample characterized in Fig. 4, it becomes clear that the Pt-O contribution detected for the former does not originate from incomplete reduction. If a temperature of 663 K is sufficient to fully reduce the catalyst, this should also be the case at 703 K. Temperature programmed reduction experiments confirmed that the catalyst is fully reduced at 663 K.

Fourier transformed EXAFS spectra of the catalyst in its oxidised state are shown in Fig. 6. The corresponding structural parameters from the fitting procedure (Table 5) demonstrate that the peak in the spectra at around 1.8 Å can be well represented just in terms of a Pt-O contribution. The resulting Pt-O distance is 2.04 Å, with a coordination number of 5.1. A comparison of the Pt-O distance of the oxidised catalyst (2.04 Å) with the one obtained from the catalyst after "direct reduction" (2.25 Å, Table 3) points out that different kinds of Pt-O bonds are involved. Upon oxygen chemisorption on reduced Pt/SiO$_2$ at 298 K,

TABLE 5

EXAFS Structural Derived from the Data in Fig. 6

Absorber	Backscatterer	CN[a]	$\Delta\sigma^2$	R/Å
Pt	O	5.1	0.0011	2.04

[a] Coordination number.

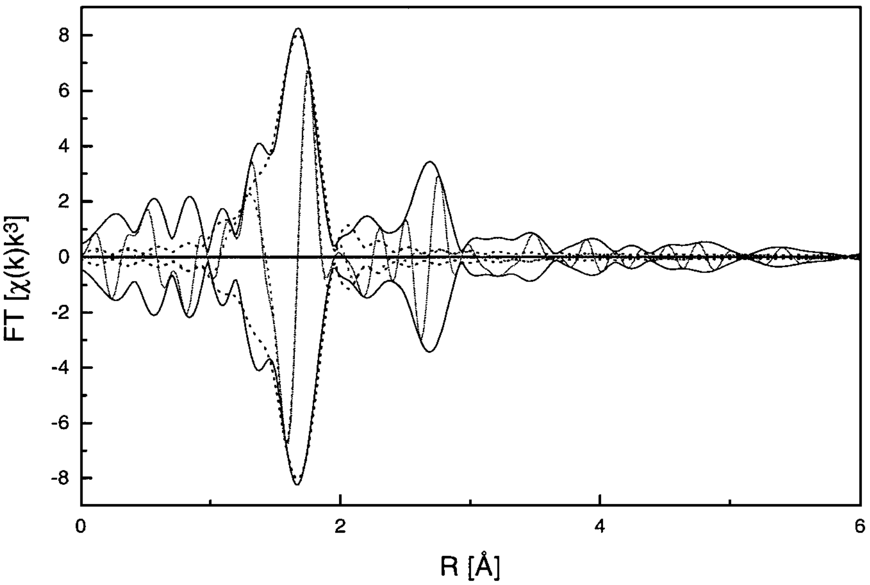

FIG. 6. EXAFS spectra of the oxidised Pt A catalyst (solid line). A fit in terms of a Pt-O contribution derived from the $Na_2Pt(OH)_6$ reference sample is shown as the dotted line.

Lytle *et al.* (27) have determined a metal–oxygen distance of 2.03 Å, which is suggested to be the Pt-O distance for surface oxygen on the metal. Hence, the longer metal–oxygen distance after direct reduction cannot be explained by surface oxygen on the metal. According to Vaarkamp *et al.* (19) the longer Pt-O distance can be attributed to a characteristic interaction of zero-valent platinum in contact with an oxide support. In their EXAFS measurements, Vaarkamp *et al.* found two different Pt-O distances depending on the reduction temperature, a short one at 2.2 Å and a longer one at 2.6–2.7 Å. The authors suggest that both distances originate from metal–support bondings. The shorter distance is ascribed to direct contact of the metal with the support oxygen, while in the other case interfacial hydrogen causes the longer bond of platinum and oxygen. This leads to the conclusion that at higher reduction temperatures interfacial hydrogen is irreversibly removed. In the present study, only the shorter $Pt\text{-}O_{support}$ distance (2.25 Å) could be detected, while any longer distance, if present, could not be extracted from the data due to overlap with Pt-Pt coordination peaks.

Catalytic Tests

The mentioned structural changes occurring at the metal–support interface during high reduction temperatures lead one to expect severe influence on the catalytic properties of the catalyst. This is confirmed by methylcyclohexane dehydrogenation tests with catalysts tubes subject to the different pretreatments, as described in more detail elsewhere (25). For catalyst A pretreated by direct reduction at high temperature, Figs. 7 and 8 show the temperature dependence of the toluene yield at 7 and 2 bar absolute,

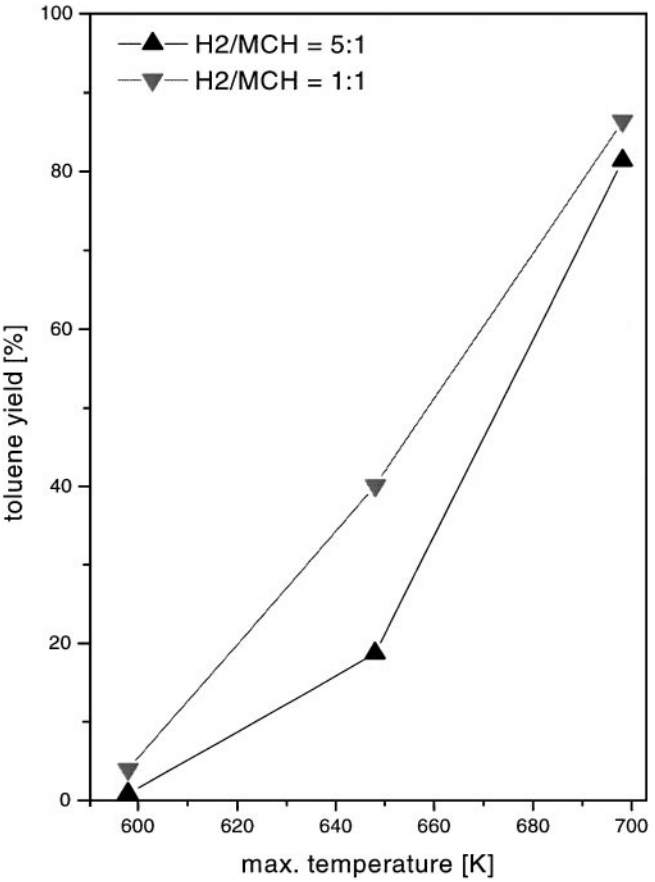

FIG. 7. Dehydrogenation experiment at 7 bar absolute. Temperature dependent toluene yields are shown for catalyst Pt A after direct reduction at 703 K.

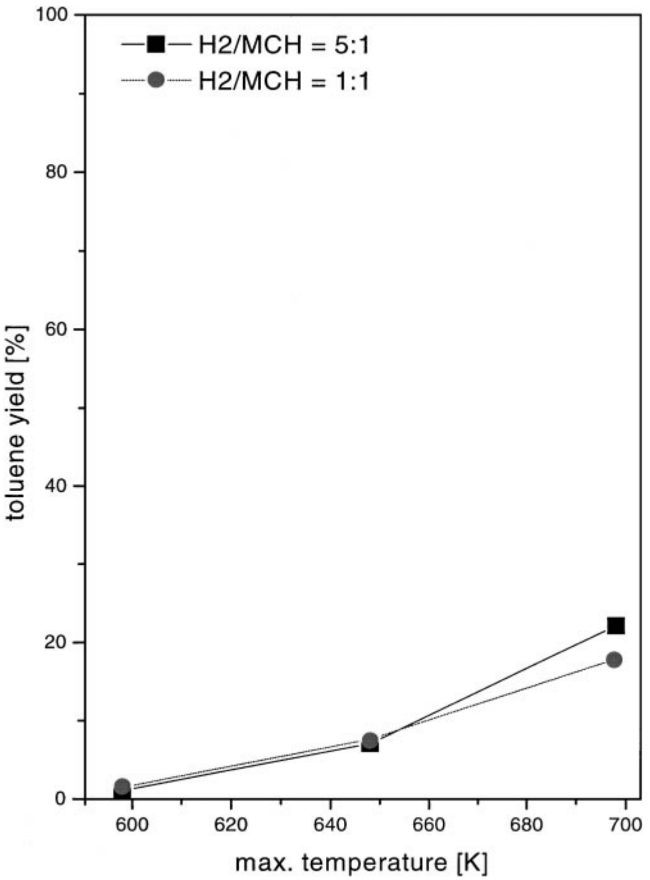

FIG. 8. Dehydrogenation experiment at 2 bar absolute. Temperature dependent toluene yields are shown for catalyst Pt A after direct reduction at 703 K.

respectively. At 7 bar the maximum yield is ≈90%, while at 2 bar only 20% was achieved.

For the corresponding experiments after mild pretreatment of catalyst A, Figs. 9 and 10 show the toluene yield at 7 bar and 2 bar absolute, respectively. For both pressures, a significant rise in activity was observed as compared to the former pretreatment, with toluene yields higher than 98% for the maximum temperature. These tests demonstrate clearly that the stronger metal–support interaction after high reduction temperatures has a considerable adverse effect on the catalytic activity of the catalyst. This phenomenon was previoulsly suggested by Vaarkamp (20) and also remarked by den Otter and Dautzenberg (29) after catalyst reduction at 823 K in the catalytic conversion of *n*-hexane.

CONCLUSIONS

The examined platinum, platinum/rhenium, and platinum/tin catalysts with aluminium oxide support are characterised by type-IV nitrogen adsorption isotherms, indicating mesopores with a average diameter of 9 nm and a BET surface area between 178 m^2/g and 197 m^2/g.

For the platinum catalyst (with the lower Pt loading) a good dispersion was found with CO chemisorption, whereas the bimetallic catalysts exhibited low dispersion values due to the mild reduction temperature used in the pretreatment. A comparison of the data from XPS and ICP-AES leads to the conclusion that for the bimetallic catalyst, an enrichment of rhenium or tin at the surface is taking place. This fact also accounts for the low platinum dispersion values.

CO chemisorption, HRTEM and EXAFS experiments for the low-loaded platinum catalyst resulted in good agreement with respect to the particle sizes. A dispersion value between 75% and 80% was obtained, with an average cluster size of 30 atoms and a particle diameter around 13 Å.

EXAFS measurements of catalysts reduced in hydrogen at 703 K revealed a peak in the spectra corresponding to a Pt-O contribution with a distance of 2.25 Å. This Pt-O contribution is due to a stronger interaction between the metal and the support. According to literature, this type of coordination arises after loss of interfacial hydrogen at higher reduction temperatures. After a mild pretreatment

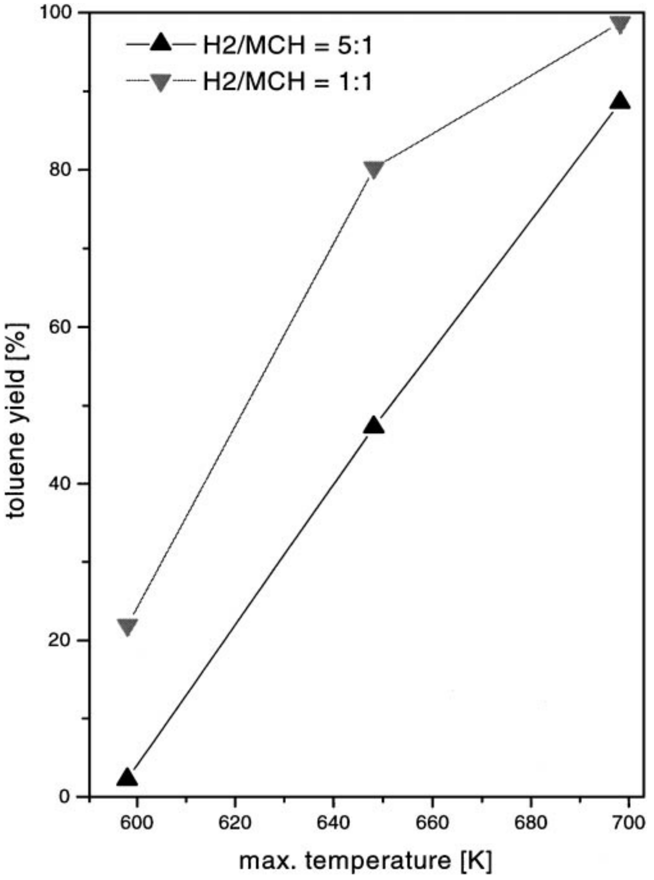

FIG. 9. Dehydrogenation experiment at 7 bar absolute. Temperature dependent toluene yields are shown for catalyst Pt A after a mild pretreatment at 663 K.

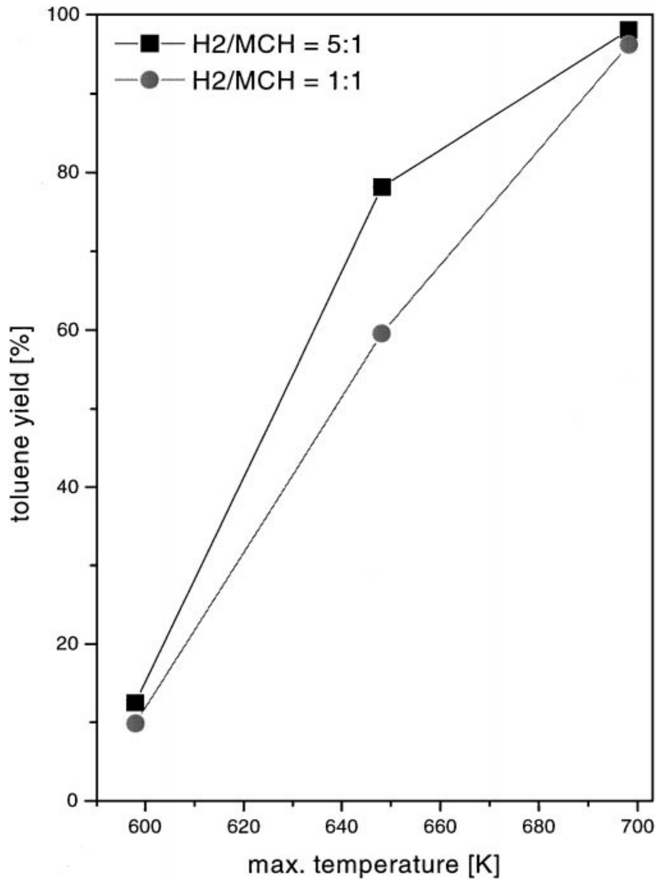

FIG. 10. Dehydrogenation experiment at 2 bar absolute. Temperature dependent toluene yields are shown for catalyst Pt A after a mild pretreatment at 663 K.

at 663 K no such peak was detected. Tests of methylcyclohexane dehydrogenation after both kinds of pretreatment showed that the stronger metal–support interaction exerted a negative influence on the catalytic activity. Toluene yields after the mild pretreatment were considerably higher than after the reduction at higher temperatures.

ACKNOWLEDGMENTS

Thanks are due to E. Newson for his guidance in the catalytic experiments, which are reported more fully at another place (25). We are indebted to the European Synchrotron Radiation Facility, Grenoble, France, and to the Swiss Norwegian Beamline collaboration SNBL for granting us access to the beamline and the laboratory. Financial support of this work by the Nationaler Energie-Forschungs-Fonds (NEFF) is gratefully acknowledged.

REFERENCES

1. Eklund, G., and v. Krusenstierna, O., *Int. J. Hydrogen Energy* **8**, 463 (1983).
2. Giacomazzi, G., Gretz, J., and Paruccini, M., Haus der Technik, Vortragsveröffentlichung., 528 (1987).
3. Cacciola, G., Giordano, N., and Restuccia, G., *Int. J. Hydrogen Energy* **9**, 411 (1984).
4. Andreassen, K., Bünger, U. H., Henriksen, N., Øyvann, A., and Ullmann, O., *Int. J. Hydrogen Energy* **18**, 325 (1993).
5. Gretz, J., Baselt, J. P., Ullmann, O., and Wendt, H., *Int. J. Hydrogen Energy* **15**, 419 (1990).
6. Taube, M., and Taube, P., *in* A liquid organic carrier of hydrogen as fuel for automobiles, "3rd World Hydrogen Energy Conference, Tokyo." Pergamon Press, Oxford, 1980.
7. Manser, R. H., Ph.D. thesis, ETH Zurich, No. 9996, Zurich, 1992.
8. Haueter, T., Maria, G., and Newson, E., Paul Scherrer Institut, TM-51-96-05 (1996).
9. Bournonville, J.-P., Chaouki, J., Touzani, A., Klvana, D., and Bélanger, G., *Rev. Inst. Francais Pétrol* **43**, 873 (1988).
10. Garland, M., Baiker, A., and Wokaun, A., *Ind. Eng. Chem. Res.* **30**, 440 (1991).
11. Müller, S., Ph.D. thesis, ETH Zurich, No. 11160, Zurich, 1995.
12. Gates, B. C., Katzer, J. R., and Schuit, G. C., "Chemistry of Catalytic Processes," Chap. 3. McGraw-Hill, New York, 1979.
13. Dalai, A. K., and Bakhshi, N. N., *Can. J. Chem. Eng.* **70**, 269 (1992).
14. Cimini, F., and Prins, R., *Physica B* **208/209**, 699 (1995).
15. Cimini, F., Ph.D. thesis, ETH Zurich, No. 11950, Zurich, 1996.
16. Sing, K. S. W., Everett, D. H., Haul, R. A. W., Moscou, L., Pierotti, R. A., Rouquérol, J., and Siemieniewska, T., *Pure Appl. Chem.* **57**, 603 (1985).
17. Isaacs, B. H., and Petersen, E. E., *J. Catal.* **77**, 43 (1982).
18. Yacaman, M. J., and Gomez, A., *Appl. Surf. Sci.* **19**, 348 (1984).
19. Pérez, O., Romeu, D., and Yacaman, M. J., *J. Catal.* **79**, 240 (1983).
20. Vaarkamp, M., Mosica, F. S., Miller, T., and Koningsberger, D. C., *J. Catal.* **144**, 611 (1993).
21. Shido, T., and Prins, R., *J. Catal.*, submitted.
22. Kip, B. J., Duivenvoorden, F. B. M., Koningsberger, D. C., and Prins, R., *J. Catal.* **105**, 26 (1987).
23. Mieville, R. L., *J. Catal.* **87**, 437 (1984).
24. Wagstaff, N., and Prins, R., *J. Catal.* **59**, 434 (1979).
25. Tschudin, S., and Newson, E., in press. [Tschudin, S., Ph.D. thesis, ETH Zurich, 1997.]
26. Caballero, A., Villain, F., Dexpert, H., LePeltier, F., and Lynch, J., *J. Chem. Soc. Faraday Trans.* **89**, 159 (1993).
27. Caballero, A., Villain, F., Dexpert, H., Lepeltier, F., Didillon, B., and Lynch, J., *Catal. Lett.* **20**, 1 (1993).
28. Lytle, F. W., Greegor, R. B., Marques, E. L., Sandstrom, D. R., Via, G. H., and Sinfelt, J. H., *J. Catal.* **95**, 546 (1985).
29. Otter, G. J. D., and Dautzenberg, F. M., *J. Catal.* **53**, 116 (1978).